

# Detection of Artery Section Area Using Artificial Immune System Algorithm

KAMIL ŘÍHA<sup>1</sup>, PENG CHEN<sup>2</sup>, DONGMEI FU<sup>2</sup>

<sup>1</sup> Department of Telecommunications  
Brno University of Technology  
Purkyňova 118, 612 00 Brno  
CZECH REPUBLIC

<sup>2</sup> Automation Department  
University of Science and Technology Beijing  
Xueyuan Road No. 30, 100083 Beijing  
P. R. CHINA

**Abstract:** - This article presents the complete chain of a method for the detection of artery section area in its perpendicular cut. The main components of the complete method are the Hough transformation for the detection of initial circle parameters and the method of discrimination-based artificial immune system for the classification of pixels located inside and outside of the artery. The source image for this processing procedure is an ultrasound B-mode picture. The main goal of this work is to find the curve of the heart cycle of blood pressure in an ultrasound video-sequence which contains a short sample (a few seconds) of pulsating geometric dimensions of the carotis comunis artery in time.

**Index Terms:** - Hough Transformation, Discrimination Based Artificial Immune System, Artificial Lymphocyte, Ultrasound Image, Cardiac Curve

## 1 Introduction

There is a great interest in medical non-invasive display and analysis of internal organs and, in particular, biological processes inside the human body. One of them is the area of blood circulation system diagnostics with focus on the analysis of dynamic blood-pressure parameters [1]. In the light of this work, we are searching for a method for detecting the inner part of artery and for computing the changes in its area during the video-sequence. The resultant curve provides good source data for finding a correlation between the geometric dimensions of the artery and the blood pressure.

There are two main possibilities of source data acquisition: longitudinal and perpendicular cuts of the artery being scanned. Both these sources have their own features and require therefore their own processing procedure. This article deals with the second of them (see Fig. 1, sized 540×480 pix) with the main feature – artery circle – as a reference for a rough classification of data in

dependence on its location: inside or outside the scanned artery.

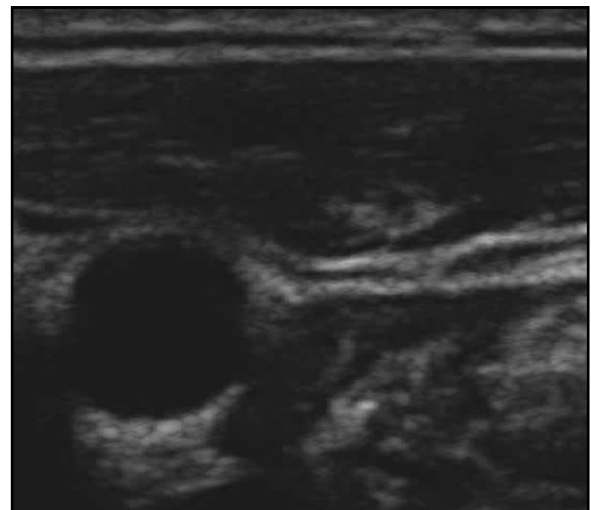


Fig. 1 Perpendicular cut of an artery in ultrasound image.

For this reason, the Hough transformation method is

used to detect the centre and radius of initial circle. On this basis we can then teach the second method, the Discrimination Based Artificial Immune System method [2], to perform a fine classification of pixels in every frame. After this, the final result is computed, i.e. the curve of the number of pixels denoted as being inside of the artery for every frame (time sample) in the video-sequence.

## 2 Hough Transformation for Circle Detection

The main goal of this stage is to denote the pixels in the reference image (the first image in a sequence) potentially being roughly inside the artery circle. Here we can make use of the fact that the inner part of the artery (blood) is *anechoic* (i.e. without ultrasound reflections) and so almost black. In contrast to this, the artery wall is *hyperechoic* (i.e. with strong ultrasound reflections) and thus almost white. Therefore, there is an easily detectable edge between the inner and the outer artery part.

### 2.1 Histogram Equalization

This simple method is the first logical step because it does not need setting any parameters and increases the contrast of the dynamic range of source image histogram. This is a simple computation of the  $k$ -th level of output intensity  $s_k$ , using transformation  $T(r_k)$  of  $k$ -th level of input intensity  $r_k$ :

$$s_k = T(r_k) = \sum_{i=0}^k \frac{n_i}{n} \quad \text{for } k = 0, 1, \dots, L-1, \quad (1)$$

where  $n_i$  is the number of source image pixels with  $i$ -th intensity level, and  $n$  is the total number of pixels.

### 2.2 Median Filtering

Now we have to remove noise from the image being processed, and ensure that there will be no small parts of this equalized image with isolated intensities. This can be done by blurring the image, using the well-known procedure of filtering: median filtering with a square convolution kernel of  $13 \times 13$  in size.

### 2.3 Iterative thresholding

The final result of the first stage is denoting (in the form of binary image) areas where the intensity is of very low level, and the other areas. Hence, this is the right moment for thresholding, using an iterative scheme [3] that has the following steps:

1. Threshold  $t_0$  is computed as an average value of image intensity function  $f(x, y)$ .
2. We get 2 groups of pixels:  $g_1$  for  $f(x, y) < t_i$  and  $g_2$  for  $f(x, y) \geq t_i$ .
3. Computation of the averages of intensity  $\overline{g_1}$  and  $\overline{g_2}$ .
4.  $t_i = 0.5 \cdot (\overline{g_1} + \overline{g_2})$ .
5. If  $\text{abs}(t_i - t_0) > \varepsilon$  then jump to step 2 and  $i = i + 1$  else finish.

The maximum number of iterations is limited to  $i \leq 100$  and the  $\varepsilon$  parameter is set experimentally. After ending this iterative process, we can perform image thresholding and get a partial binary result, see Fig. 2.



Fig. 2 Partial result after iterative thresholding step.

### 2.4 Dilating

As Fig. 2 shows, there are many candidate centres (black) after thresholding. To reduce their number, we can use the method of dilation formulated for binary image by the equation

$$A \oplus B = \{z | [(\hat{B})_z \cap A] \subseteq A\}, \quad (2)$$

where  $A, B$  are sets in  $Z^2$ ,  $z = (z_1, z_2)$  is a point,  $\hat{B}$  is a reflection of  $B$  about its origin, and  $(B)_z$  is the translation of set  $B$  into point  $z$  [3]. The result of this equation can be seen as a set of all displacements of (the origin of) reflected set  $B$  to a point  $z$  if  $\hat{B}$  and  $A$  are intersected in at least one element.  $B$  is the so called *structuring element* (kernel), here an element of  $3 \times 3$  in size is used.

Dilation is an iterative process. Based on experimental results, the sufficient number of iteration was determined as 35. As the results show in Fig. 3, the number of candidate centres is strongly reduced after dilation iterations.

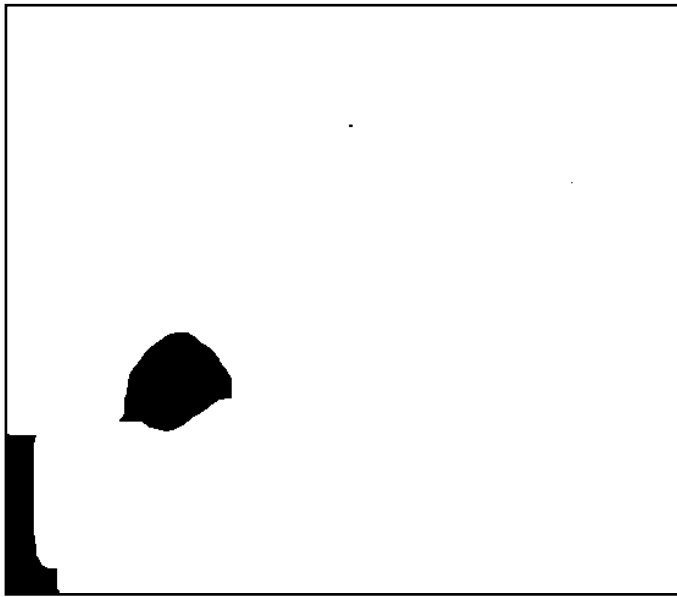


Fig. 3 Partial result after iterative dilating step – candidate centres.

## 2.5 Hough transform

The above-mentioned candidate centres are one half of the most important source data for the Hough transformation. The second half can be simply extracted from image after thresholding (Fig. 2) by detecting the binary edges. These bright points - candidate points located on the perimeter of a circle - can be seen in Fig. 4.

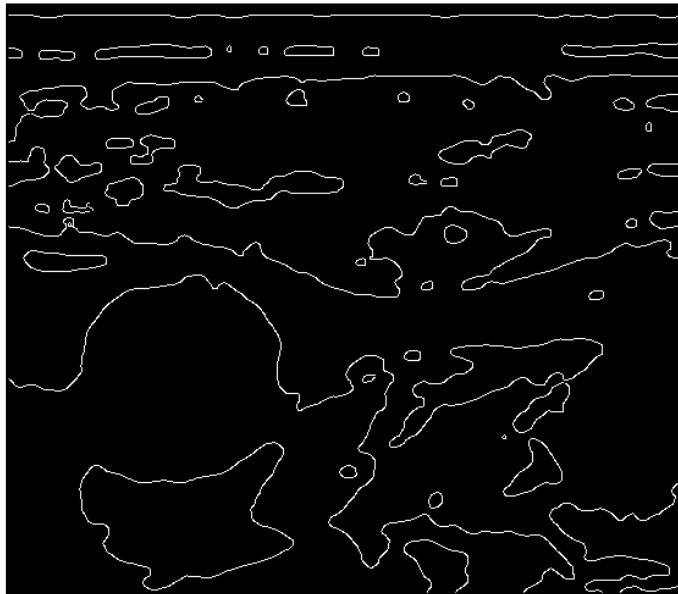


Fig. 4 Partial result after edge detection – candidate perimeter points.

The Hough transformation becomes a 3D problem, because we need 3 parameters for the definition of 1 circle: two coordinates of centre  $(x_n, y_n)$  and radius  $r_n$ . However,

we have the possibility to change it into a 2D problem, because we can interpret the 2D coordinate pairs of candidate centres as a set of 1D points. We can analytically formulate the appropriate radius for every such point, which means a definition of special parametric space (see Fig. 5).

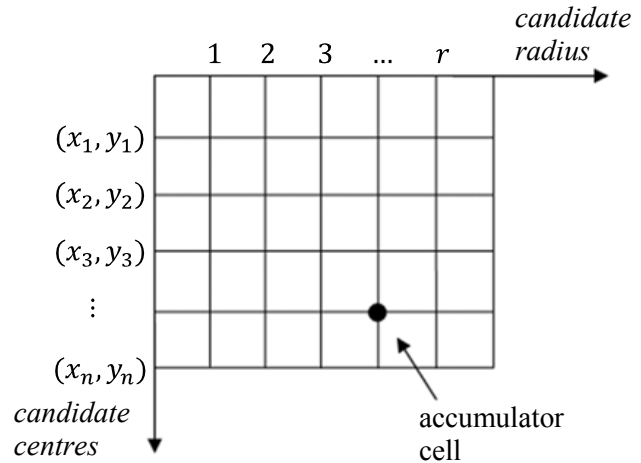


Fig. 5 Hough transformation parametric space for circle detection.

Now we have prepared the data of candidate points: the coordinates of candidate centres  $(x_n, y_n)$  and the coordinates of candidate perimeter points  $(x'_n, y'_n)$ . Moreover, we have here a radius  $r_n$ , which is given for each pair of these points by the equation

$$r_n^2 = (x'_n - x_n)^2 + (y'_n - y_n)^2. \quad (3)$$

All these parameters define  $n$  potential initial artery circles.

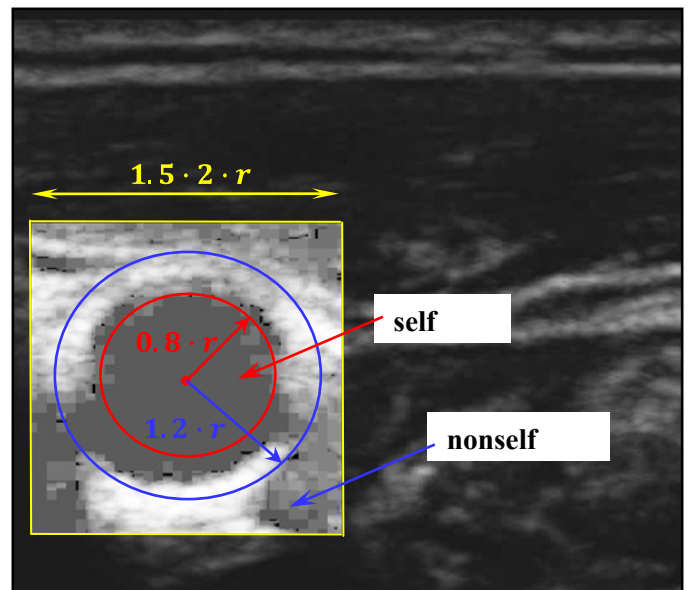


Fig. 6 Dividing source data based on initial circle parameters.

The task for the Hough transformation is to increment the appropriate accumulator cell on a parametric space coordinate calculated by eq. (3) for all coordinates of candidate centres and candidate perimeter points. After processing all points  $(x_n, y_n)$  and  $(x'_n, y'_n)$ , the sought initial circle parameters can be founded in the accumulator of the Hough transformation parametric space as a cell with maximum value.

Based on the initial circle parameters we can now reduce the analyzed area to a square of  $1.5 \cdot \text{diameter}$  of initial circle in size and with identical centres. The reduced window with equalized histogram is shown in Fig. 6, together with other important parameters described in the following chapter.

### 3 Artificial Immune System Classification Algorithm

#### 3.1 Dividing the Data

We have only initial circle parameters, after the Hough transformation step for the first (reference) frame in the video-sequence. This is a good starting point for the application of a method that will finally denote the area inside and outside of the artery. For this purpose, the Discrimination-Based Artificial Immune System (DAIS) method [2] is used.

What we actually need is to acquire easily divisible features of both areas inside and outside of the artery: *self* and *nonself* data sets respectively. For this purpose, the two-dimensional feature space is convenient. This space needs to define two features of analyzed data: in our approach we have used histogram-equalized ( $i_H$ ) and median-filtered ( $i_M$ ) image intensities, as can be seen in Fig. 7.

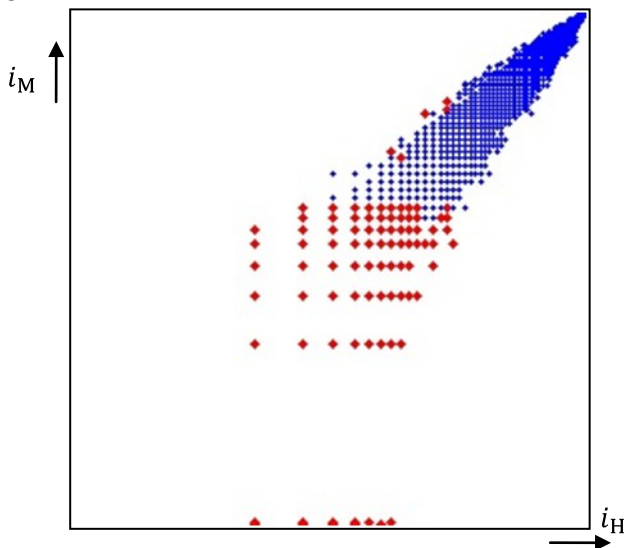


Fig. 7 Division of source data based on initial circle parameters.

The first step of DAIS is a rough division of source data into two basic groups for training Artificial Lymphocyte Cells (ALC, see the next chapter), because the concept of DAIS is based on the self-nonsel discrimination principle of lymphocytes in the human immune system, which are able to discriminate between self and nonself molecules in the human body.

First, we need to perform a rough and reliable division of features into self and nonself sets based on the result of the Hough transformation – initial circle. As Fig. 6 shows, we can get the coordinates of individual elements of sets by considering their position inside a circle of  $\text{radius} = 0.8 \cdot r$  ( $r$  is the radius of initial circle). The nonself group is defined by pixels whose coordinates lie outside a circle of  $\text{radius} = 1.2 \cdot r$ , and the intensity level is higher than 80 (determined experimentally). Of course, only elements in the analyzed area of square size equal to  $3 \cdot r$  are considered. In Fig. 7 we can see two data sets in 2D feature space without information about their spatial position, containing only their two intensity features  $i_H$  and  $i_M$ . The red colour represents the self elements and the blue colour the nonself elements of the data set.

#### 3.2 Artificial Lymphocyte Cell

The Artificial Lymphocyte Cell is a mathematical model of a natural lymphocyte trained in thymus to achieve the required ability: it has to react with (recognize) nonself elements and not to react with self elements. In the sense of [2] we can define the ALC as a nonself data set element (pair of intensity features) coupled with the so called *RDT* (Recognition Distance Threshold) computed as

$$RDT = D_{\min} \cdot \alpha, \quad (4)$$

where  $\alpha$  is a constant set experimentally in the range  $0 < \alpha < 1$  and  $D_{\min}$  is the minimum distance to the self data element. Now we consider the term “distance”  $D$  as a Euclidean distance between the data elements in feature space:

$$D = \sqrt{i_H^2 + i_M^2}. \quad (5)$$

The demonstration of *RDT* meaning is illustrated by Fig. 9. The *RDT* circle means an area in the 2D feature space where the ALC will recognize nonself elements. A larger area means a higher ALC effectiveness, because it is able to cover a larger area of occurrence of nonself elements in the feature space.

An interesting description of ALC characteristic is the so called *affinity* 0:

$$\text{affinity} = \sqrt{RDT^2 + \text{nonselfNum}^2}, \quad (6)$$

where *nonselfNum* is the amount of nonself class

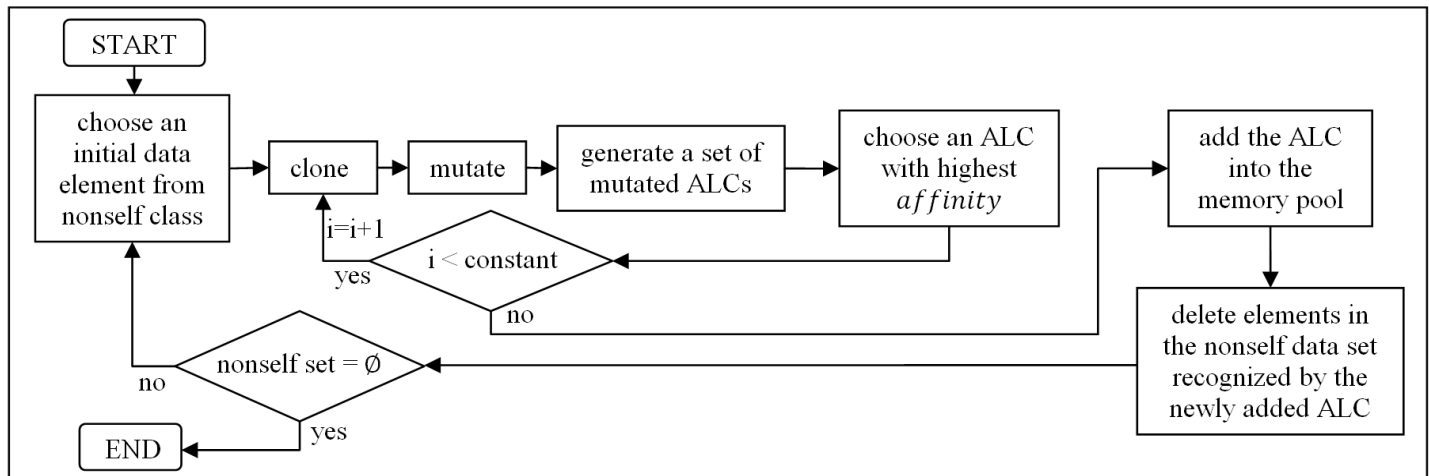


Fig. 8 Flow chart of procedure for ALCs generating.

elements recognized (overlaid) by the appropriate ALC. This parameter will be important for the ALC training chain described in the next chapter.

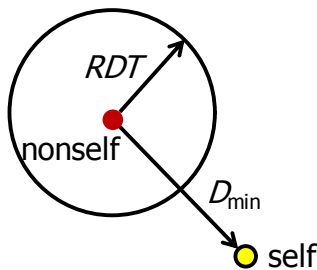


Fig. 9 The meaning of the ALC in 2D feature space.

### 3.3 Learning Algorithm for ALCs

The goal of ALCs is to cover (detect) all the elements lying in the nonself class. Because two groups of data in the feature space are not located in the formation with circular shape, a certain number of ALCs will be needed for covering the whole nonself training class. For that reason, a *memory pool* of the necessary ALCs has to be created by a process called *Learning Algorithm*, which is an analogy to the thymus function in the human body for training live lymphocytes.

A simplified flow-chart of this procedure is given in Fig. 8. In the first step, the initial memory cell from the nonself data set is randomly selected. These data are then *cloned* in a given amount (determined experimentally) and these clones are then *mutated*, which means that their values are changed on the basis of a random number, whose influence on the change of value can, in addition, be set after experiments. Pairs of mutated values are then complemented with their corresponding *RDTs*. This triad is a complete ALC, for which the parameter *affinity* can be computed and evaluated. The ALC with the highest

*affinity* is selected and the process is repeated with these selected ALC data from the cloning step. After a given number of iterations the output ALC with the highest affinity is then saved in the memory pool and the nonself class data are reduced by the elements that the newly added ALC is able to detect. This process is repeated until the nonself class is empty.

Now we can select the nonself class, which can be made up of different sub-classes. The intended result - self data set, interior artery area - is identified in the sense of *negative selection*.

### 3.4 Negative Selection

The final step of the DAIS algorithm is the selection of a self class of data using the trained ALCs. This is done by the negative selection technique, whose simplified flow-chart can be seen in Fig. 10.

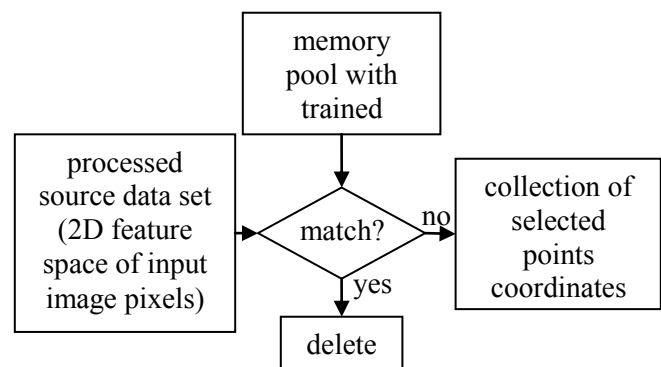


Fig. 10 The simplified flow-chart of negative selection.

Fig. 10 shows the selecting procedure, which is repeated for each pixel from source data. The “match?” decision means examining whether distance  $D$  of the input feature point being processed is less than *RDT* of the given ALC. If one of the ALCs recognized a data point, then the point

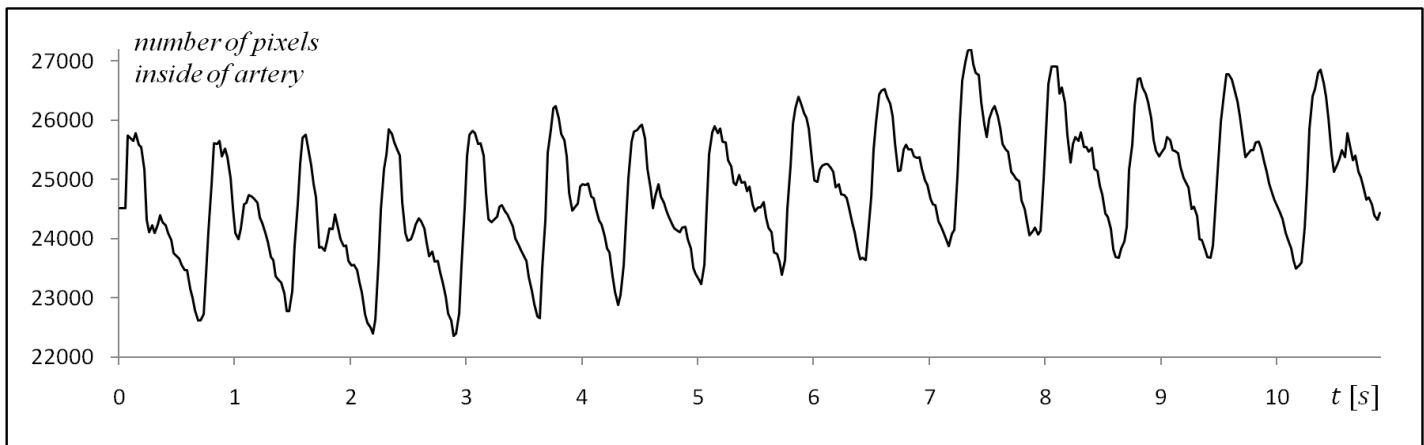


Fig. 11 The final cardiac curve.

can be classified as nonself and can be deleted from the whole group of source feature points. Hence, there are only self data elements remaining at the end of this procedure.

The graphical illustration of a negative selection example in the 2D feature space (for one frame in the video-sequence) with ALC circles (with centres and *RDT* perimeters in black colour) can be seen in Fig. 12.

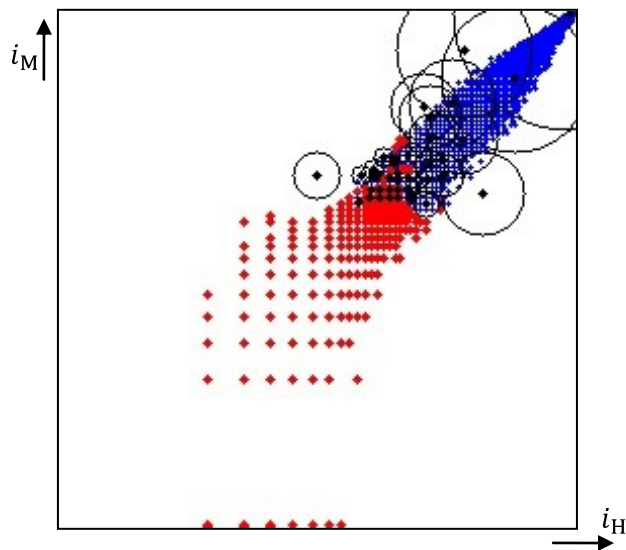


Fig. 12 The negative selection procedure in an example of feature space.

## 4 Experimental Results

After the application of all the aforesaid processing steps we can embark on the final procedure of extracting the numbers of pixels located inside of the ultrasound image of a perpendicular artery cut. As was mentioned in the introduction chapter, we need to get some information about the area inside of the artery in order to analyze time variations of artery in comparison with blood pressure,

which will be the subject matter of a future work falling into the area of biomedical methods. Fig. 11 shows the result of a part of image processing of the problem solved: the inner part of artery cross-section, expressed in terms of the number of pixels located within the artery circle, in dependence on time. The time is derived from the FPS of a given video-sequence, which is equal to 43 frames per second.

The ultrasound video-sequence was acquired on a volunteer's *carotis comunis*, using the Sonix OP Smart Ultrasound system with linear probe at 14.0 MHz.

## 5 Conclusion

The method of image processing for the measuring of the inner area of artery was presented. The method uses the Hough transformation and clonal selection as the main methods for artery circle detection and inner/outer artery part classification. The image processing chain is applied to every single frame in the video-sequence and the output numbers of inner artery area pixels form the time-dependent cardiac curve which is prepared for correlative analysis with blood pressure. The main aim for the future is to use the resulting image processing method in biomedical research.

### Acknowledgement:

This work was prepared with the support of the MSMT project No. 2B06111 and the FRVS project No. 1261/2008.

## References:

- [1] ŘÍHA, K.; ČÍŽ, R.: Searching for a New Non-invasive Method of Blood Circulation System Diagnostics. In *The Third International Conference on Systems*, ICONS 2008. Cancun, Mexico, 2008. ISBN 978-0-7695-3105-2.
- [2] KAZUSHI IGAWA; HIROTADA OHASHI: A Discrimination Based Artificial Immune System for Classification. In *Proceedings of the International Conference on Computational Intelligence for Modelling, Control and Automation and International Conference on Intelligent Agents, Web Technologies and Internet Commerce Vol-2*, IEEE Computer Society 2005, ISBN:0-7695-2504-0-02.
- [3] GONZALEZ, R. C.; WOODS, R. E., *Digital Image Processing*, Prentice Hall, New Jersey, 2002.
- [4] GARAIN, U.; CHAKRABORTY, P. M.; DASGUPTA, D.: Recognition of Handwritten Indic Script using Clonal Selection Algorithm. In *Artificial Immune Systems Vol-4163/2006*, Springer Berlin / Heidelberg. ISBN 978-3-540-37749-8.
- [5] IOANNOU, D.; HUDA, W.; LAINE, F. A.: Circle Recognition Through A 2D Hough Transform And Radius Histogramming. In *Image and Vision Computing Vol-17*, Elsevier Science B. V., DOI: 10.1016/S0262-8856(98)00090-0.
- [6] THEODORIDIS, S.; KOUTROUMBAS, K.: *Pattern Recognition*, Academic Press, San Diego, 2003.
- [7] ZHOU, J.; DASGUPTA, D.: Revisiting Negative Selection Algorithms. In *Evolutionary Computation Vol-15*, MIT Press, ISSN 1063-6560.